In Vivo Architecture and Action of Bacterial Structural Maintenance of Chromosome Proteins

Anjana Badrinarayanan *et al.*

Science **338**, 528 (2012);
DOI: 10.1126/science.1227126

Science (print ISSN 0036-8075; online ISSN 1095-9203) is published weekly, except the last week in December, by the American Association for the Advancement of Science, 1200 New York Avenue NW, Washington, DC 20005.

The strength of the phenotype may thus be influenced by the relative incorporation of Env variants. This view is consistent with the finding that the Env(ΔCT) variant shows a cell-type–dependent infectivity defect (*3*, *22*), which correlates with Env incorporation and can be rescued by a mutation that increases this incorporation (*25*).

We suggest that Env trimers are initially recruited to viral budding sites in a random distribution, yielding a multifocal appearance. Their lateral movement is restricted by the underlying rigid Gag lattice interacting with the Env CT and preventing formation of a single Env cluster in the immature virus. Proteolytic maturation, specifically the separation of MA from CA, overcomes this restriction, leading to coalescence into a single Env focus, driven by intermolecular Env CT interactions. This rearrangement polarizes the virus particle with subsequent attachment of the Env cluster to a CD4 patch on the target cell surface, thus initiating virus entry. Whereas Env trimers with truncated CT are mobile irrespective of Gag maturation, they lack the propensity to cluster. Clustering of Env trimers is partially rescued upon engagement of the cellular receptor provided that individual trimers are free to move within the viral membrane. Conversion of the inner core is thereby coupled to surface alterations in a mechanism of "inside-out signaling," ensuring that only particles whose interior has switched to the entry mode are fully competent for membrane fusion.

References and Notes

1. P. Cosson, *EMBO J.* **15**, 5783 (1996).
2. E. O. Freed, M. A. Martin, *J. Virol.* **70**, 341 (1996).
3. T. Murakami, E. O. Freed, *Proc. Natl. Acad. Sci. U.S.A.* **97**, 343 (2000).
4. E. Chertova *et al.*, *J. Virol.* **76**, 5315 (2002).
5. P. Zhu *et al.*, *Proc. Natl. Acad. Sci. U.S.A.* **100**, 15812 (2003).
6. R. H. Cheng *et al.*, *Cell* **80**, 621 (1995).
7. A. Harris *et al.*, *Proc. Natl. Acad. Sci. U.S.A.* **103**, 19123 (2006).
8. P. Zhu *et al.*, *Nature* **441**, 847 (2006).
9. A. Helenius, *Cell* **69**, 577 (1992).
10. T. Murakami, S. Ablan, E. O. Freed, Y. Tanaka, *J. Virol.* **78**, 1026 (2004).
11. D. J. Wyma *et al.*, *J. Virol.* **78**, 3429 (2004).
12. N. Kol *et al.*, *Biophys. J.* **92**, 1777 (2007).
13. S. W. Hell, J. Wichmann, *Opt. Lett.* **19**, 780 (1994).
14. A. Trkola *et al.*, *J. Virol.* **70**, 1100 (1996).
15. P. Roben *et al.*, *J. Virol.* **68**, 4821 (1994).
16. D. McDonald *et al.*, *J. Cell Biol.* **159**, 441 (2002).
17. J. A. Briggs, T. Wilk, R. Welker, H. G. Kräusslich, S. D. Fuller, *EMBO J.* **22**, 1707 (2003).
18. T. Endress *et al.*, *Eur. Biophys. J.* **37**, 1291 (2008).
19. A. de Marco *et al.*, *PLoS Pathog.* **6**, e1001215 (2010).
20. M. J. Forster, B. Mulloy, M. V. Nermut, *J. Mol. Biol.* **298**, 841 (2000).
21. S. F. Lee *et al.*, *J. Biol. Chem.* **275**, 15809 (2000).
22. T. Wilk, T. Pfeiffer, V. Bosch, *Virology* **189**, 167 (1992).
23. M. Cavrois, C. De Noronha, W. C. Greene, *Nat. Biotechnol.* **20**, 1151 (2002).
24. R. Sougrat *et al.*, *PLoS Pathog.* **3**, e63 (2007).
25. D. Holtkotte, T. Pfeiffer, T. Pisch, V. Bosch, *AIDS Res. Hum. Retroviruses* **22**, 57 (2006).
26. L. A. Carlson *et al.*, *Cell Host Microbe* **4**, 592 (2008).

Acknowledgments: We are grateful to J. Mak (Burnet Institute, Melbourne) for purified recombinant HIV-1 Gag and to P. Guardado-Calves (Institut Pasteur, Paris) for monomeric and trimeric Env gp140. We thank L. Castillo for purified recombinant HIV-1 CA, V. Bosch (DKFZ Heidelberg) for HIV-1 gp120 and CD4 antisera as well as HIV-1 Env expression plasmids, R. Doms (University of Pennsylvania) for SupT1R5 cells, C. Aiken (Vanderbilt University Medical Center) for infectious HIV-1 variant plasmids, and T. Hope (Northwestern University Chicago) for the eGFP.Vpr construct. H.-G.K. is an investigator of the Excellence Cluster CellNetworks funded by the German Research Foundation (DFG). S.W.H. holds a patent on STED microscopy in several European countries and the United States, which has been licensed to Leica, a microscope manufacturer.

Supplementary Materials

www.sciencemag.org/cgi/content/full/338/6106/524/DC1
Materials and Methods
Figs. S1 to S10
Table S1
References (*27*–*33*)

20 June 2012; accepted 6 September 2012
10.1126/science.1226359

In Vivo Architecture and Action of Bacterial Structural Maintenance of Chromosome Proteins

Anjana Badrinarayanan,[1]*† Rodrigo Reyes-Lamothe,[1]*‡ Stephan Uphoff,[2] Mark C. Leake,[2]§ David J. Sherratt[1]§

SMC (structural maintenance of chromosome) proteins act ubiquitously in chromosome processing. In *Escherichia coli,* the SMC complex MukBEF plays roles in chromosome segregation and organization. We used single-molecule millisecond multicolor fluorescence microscopy of live bacteria to reveal that a dimer of dimeric fluorescent MukBEF molecules acts as the minimal functional unit. On average, 8 to 10 of these complexes accumulated as "spots" in one to three discrete chromosome-associated regions of the cell, where they formed higher-order structures. Functional MukBEF within spots exchanged with freely diffusing complexes at a rate of one complex about every 50 seconds in reactions requiring adenosine triphosphate (ATP) hydrolysis. Thus, by functioning in pairs, MukBEF complexes may undergo multiple cycles of ATP hydrolysis without being released from DNA, analogous to the behavior of well-characterized molecular motors.

SMC (structural maintenance of chromosome) complexes share conserved architectures and function in chromosome maintenance in all domains of life, although the molecular mechanism by which they act in vivo is unknown (*1*–*3*). In eukaryotes, SMC heterodimers associate with a range of accessory proteins, acting in chromosome organization, sister chromosome cohesion, and other chromosome biology functions, whereas in bacteria an SMC homodimer and associated accessory proteins act in chromosome maintenance (*1*). In *Escherichia coli* and some other γ proteobacteria, a distant SMC relative, MukB with accessory proteins MukE and MukF, replaces the typical SMC complex but has similar functions (*4*, *5*). Bacterial *smc* null mutants are frequently temperature sensitive, produce anucleate cells, and show disturbed chromosome organization at permissive temperature, indicating roles in SMC-mediated chromosome segregation and/or compaction (*1*, *6*, *7*). In *E. coli* undergoing nonoverlapping replication cycles, MukBEF accumulates as "spots" at about one to three discrete chromosome locations, typically at mid-cell and/or quarter-cell, in the same regions as replication origins (*6*). Structural and biochemical MukBEF fragment studies report two subunit arrangements, 2:4:2 or 2:2:1, for MukB:E:F, dependent on whether adenosine triphosphate (ATP) is absent or bound, respectively (*8*) (fig. S1A). Here, our aim was to understand the molecular architecture of active SMC complexes in vivo, as well as the transformations undergone during ATP binding and hydrolysis, as complexes associate with, and dissociate from, the chromosome.

E. coli cells, in which endogenous MukBEF genes were replaced by functional yellow fluorescent protein (YPet) fusions, were analyzed by slimfield microscopy, a strategy used previously for studying replisomes (*9*) (Fig. 1A, figs. S1 and S2, and tables S1 to S3). Analysis of the numbers of MukB, E, or F molecules

[1]Department of Biochemistry, University of Oxford, UK. [2]Department of Physics, University of Oxford, UK.

*These authors contributed equally to this work.
†Present address: Department of Biology, Massachusetts Institute of Technology, Cambridge, MA 02139, USA.
‡Present address: Department of Biology, McGill University, Montreal, Quebec H3G 0B1, Canada.
§To whom correspondence should be addressed. E-mail: m.leake1@physics.ox.ac.uk (M.C.L.); david.sherratt@bioch.ox.ac.uk (D.J.S.)

in individual fluorescent spots showed broad stoichiometry distributions, even between spots in the same cell, with mean values 36 ± 3, 36 ± 4, and 19 ± 1 molecules (±SEM) for MukB, E, and F, respectively (*9*, *10*) (Fig. 1B and C). Fourier analysis showed periodicities in stoichiometry of 4:4:2 molecules, respectively, for MukB:E:F (Fig. 1C, insets). Spots were elongated parallel to the cell's long axis (Fig. 1D), suggesting that MukBEF complexes spanned several tens of nm, with a decrease of ~20% in measured spot width with increasing stoichiometry across the range measured, consistent with increasing compaction of MukBEF structures as more molecules are added (fig. S3 and table S4).

Higher-resolution data were obtained using live-cell PALM (photoactivated localization microscopy) (*11*) with functional photoactivatable red fluorescent protein (PAmCherry) fusions to MukBEF. Rapidly diffusing and relatively immobile populations forming about one to three immobile elongated spots per cell were observed, as in slimfield images (Fig. 1E), the latter resolvable into subclusters containing closely associated individual PAmCherry molecules in a diameter of less than 40 nm (figs. S4 and S5).

Slimfield analysis of diffusing cellular YPet fluorescence (*9*) (fig. S6) indicated ~300 to 400 molecules per cell for MukB and E, and ~200 molecules per cell for MukF (table S5), in broad agreement with ensemble western estimates (*12*), implying that only ~20% of cellular MukBEF is integrated into spot complexes. PALM single-particle tracking gave similar apparent diffusion coefficients for diffusing MukB, E, and F, despite large differences in individual molecular weights, compatible with their

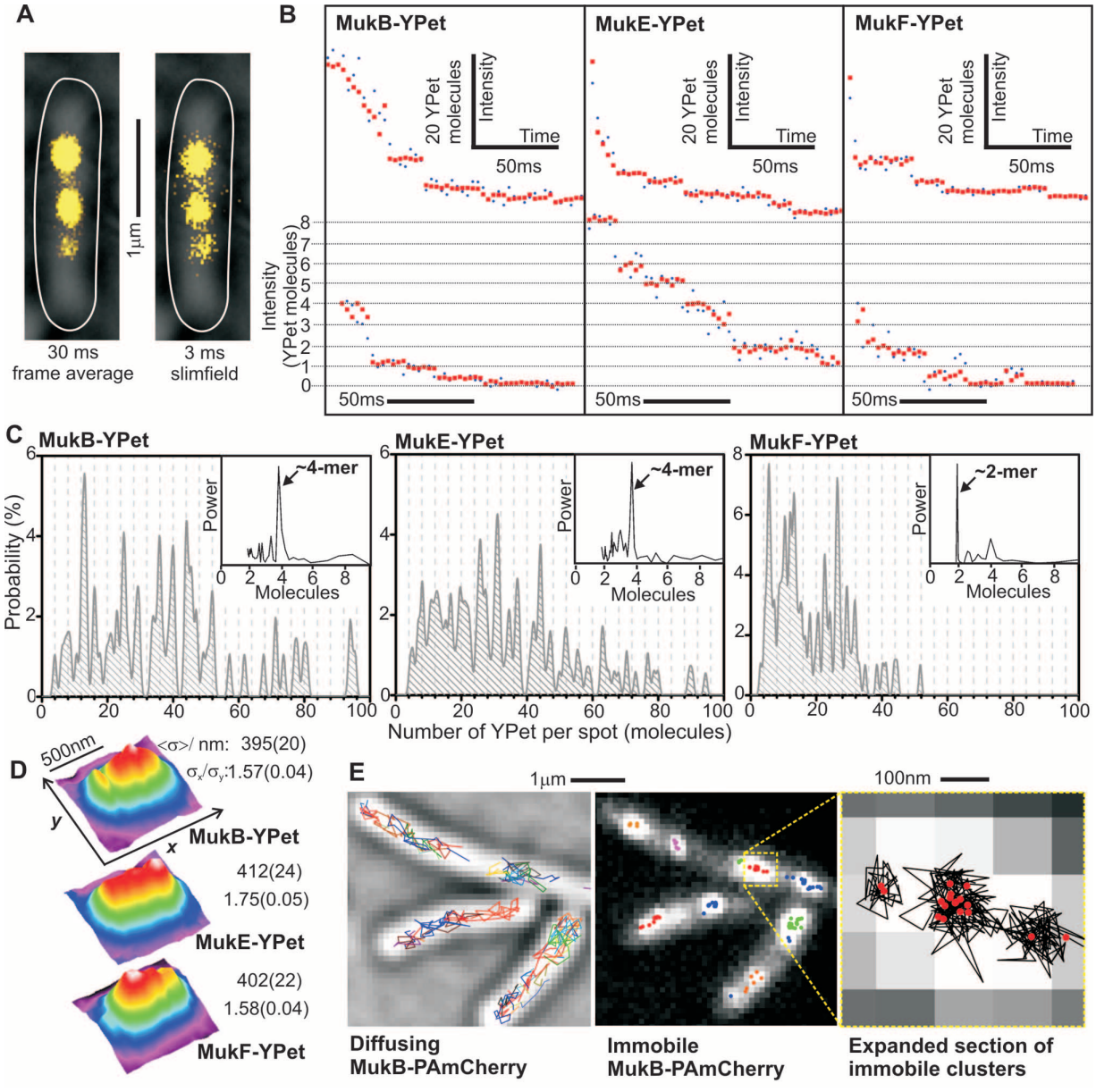

Fig. 1. MukBEF imaging. (**A**) Representative frame-average and slimfield MukB-YPet cell images (yellow), brightfield and cell outline overlaid (white). (**B**) Photobleaching of MukBEF-YPet spots, high (upper row) and low stoichiometry data (expanded sections, lower row), raw (blue) and filtered (red). (**C**) Stoichiometry distributions; N = 51 to 84 cells. Four-molecule interval grid lines, power spectra (arbitrary units) inset. (**D**) False-color plots for mean two-dimensional spatial distributions for slimfield images with a 3-ms integration time; N = 197 to 237 spots. Estimates for full width at half maximum σ and σ_x/σ_y for Gaussian fits parallel to x and y axes (SD error). (**E**) Live-cell PALM, diffusing (gray brightfield, tracks colored) and immobile MukB-PAmCherry (different clusters colored), expanded indicating tracks (black) and clusters (red).

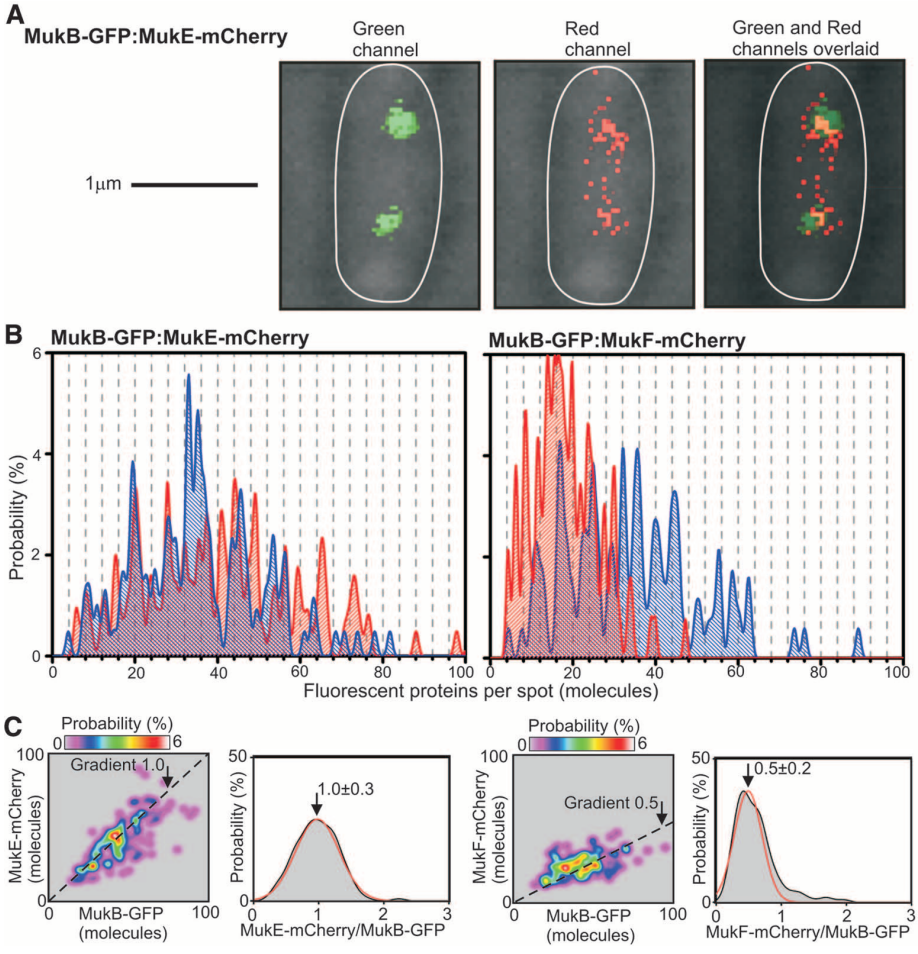

Fig. 2. Dual-color single-molecule millisecond imaging. (**A**) Brightfield (gray) and 3-ms fluorescence green (left panel) and red (middle panel) channels, overlaid (right panel) for dual-label strain. (**B**) Unbiased kernel density stoichiometry estimation on mCherry (red) and GFP (blue) components for two dual-label strains, 4-molecule spaced grid lines. (**C**) Stoichiometry of mCherry versus GFP component for each spot; dotted line gradients of 1.0 and 0.5; distribution of ratio of stoichiometry for mCherry and GFP components (gray) with Gaussian fit (red); mean ± SD indicated.

being components of the same large complexes (fig. S5).

We confirmed the stoichiometry periodicity of 4:4:2 for MukB:E:F by measuring simultaneously the intensities of mCherry and green fluorescent protein (GFP) fusions to pairs of MukB, E, and F in the same spots (Fig. 2, figs. S1 and S7, and table S6). A plot of the spot-by-spot stoichiometry gave mean ratio values of 1.0 ± 0.3 (±SD) and 0.5 ± 0.2 for relative content of MukE to MukB and of MukF to MukB, respectively. Thus, the localized MukBEF spots contain ~8 to 10 dimers of dimer 4:4:2 complexes as minimal functional units.

A 2:2:1 MukB:E:F ratio defines an ATP-bound state (*8*), resulting from displacement of one MukF and two MukE from a 2:4:2 putative ATP-free form. Given that MukF forms stable homodimers (*8*, *13*), MukF displacement may allow recruitment of a second 2:2:1 complex through MukF-mediated dimerization (*8*, *12*, *14*), generating the observed 4:4:2 periodicity. Indeed, ATP binding and MukB head engagement were essential for localized spot formation, because they were present in cells of a $MukB_{EQ}$ mutant that binds ATP but is hydrolysis-impaired (*8*, *15*, *16*), but not in cells carrying either nucleotide-binding ($MukB_{DA}$) or engagement-deficient ($MukB_{SR}$) mutations (*17*, *18*) (fig. S8). The relative stoichiometries of $MukB_{EQ}$:E:F in localized spots were similar to wild type, consistent with both being ATP-bound, as was the total number of $MukB_{EQ}EF$ complexes per spot (fig. S9), and the cellular content of diffusing molecules (tables S4 and S5). Because $MukB_{EQ}EF$ cells are Muk^{-}, MukBEF complexes must hydrolyze ATP to be functional.

To investigate whether conformational changes during ATP hydrolysis are linked to MukBEF turnover, we compared fluorescence recovery after photobleaching (FRAP) on two $MukB_{EQ}EF$ strains with wild-type counterparts (Fig. 3A and fig. S10). Detection sensitivity was increased using longer cephalexin-treated cells in which the photoactive to bleached MukBEF-YPet content was higher; recovery up to 60% of prebleach levels over several minutes was observed (Fig. 3B). In comparison, steady-state cells gave up to 30% recovery from prebleach levels (fig. S10). Reaction-diffusion modeling indicated dwell times for single MukBEF 4:4:2 complexes of ~50 s, independent of cephalexin treatment, with no dependence on prebleach intensity. Localized spots outside the original bleach zone indicated fluorescence loss in photobleaching (FLIP) over a similar time scale, converging to similar steady-state intensities. Quantifying postbleach fluorescence for all localized spots indicated ~4-molecule periodicity for MukB and MukE, and ~2-molecule periodicity for MukF (fig. S11), consistent with integer units of 4:4:2 complexes turning over. In contrast to wild-type MukBEF, $MukB_{EQ}EF$ spots showed no recovery in fluorescence after photobleaching, showing that ATP hydrolysis promoted MukBEF dissociation from DNA (Fig. 3C and fig. S10).

High-speed imaging allowed us to compare dim spots of rapidly diffusing wild-type MukBEF complexes with those carrying either ATP-binding or ATP-hydrolysis mutations. Fluorescence was converted to stoichiometries using single-molecule YPet intensity (fig. S12). Wild-type and hydrolysis mutants contained mixed populations of MukBEF complexes, with ~30% in the 4:4:2 and ~70% in the 2:4:2 state, whereas complexes of the ATP-binding mutant were exclusively in the dimeric 2:4:2 state.

Although ATP hydrolysis is essential for the activity of SMC complexes, its mechanistic importance has been unclear. Our data indicate that the minimal functional MukBEF complex acting at discrete chromosome positions is an ATP-bound dimer of MukB dimers, with ATP binding and head engagement being necessary for stable chromosome association and ATP hydrolysis required to release complexes from chromosomes. The observation

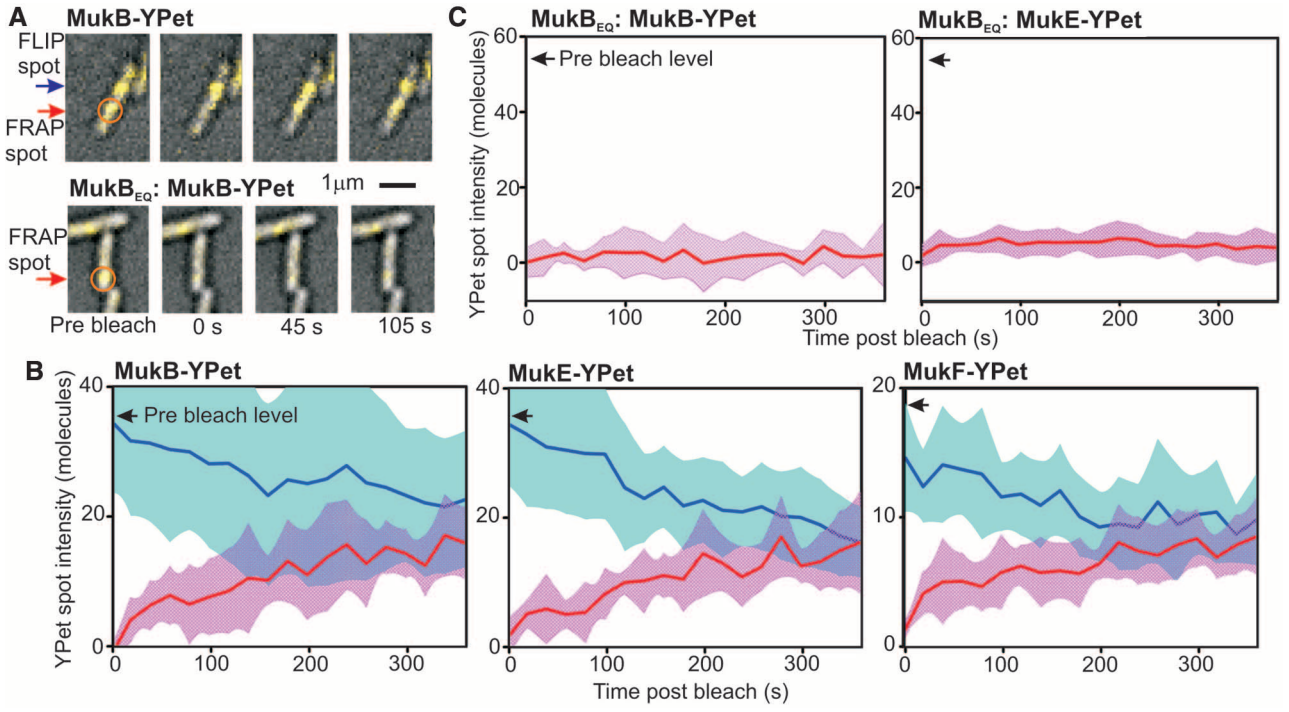

Fig. 3. Turnover of MukBEF complexes. (**A**) FRAP of MukB-YPet (upper panel) and ATP hydrolysis mutant MukB$_{EQ}$-YPet (lower panel), laser focus (orange circle), and FRAP (red arrow) and FLIP (blue arrow) indicated; steady-state cells. (**B** and **C**) Mean FRAP (red) and FLIP (blue) traces for cephalexin-elongated cells. SD errorbounds (shaded); prebleach levels shown (arrows); N = 10 to 14 traces.

that turnover of MukBEF complexes from chromosomes is slower than predicted from in vitro adenosine triphosphatase (ATPase) levels (*8*, *19*) (fig. S1F) supports a model where ATP hydrolysis within each ATPase head pair is independent, with all four ATP molecules in the two closed dimer of dimer heads needing to be hydrolyzed almost simultaneously to completely release a single DNA-bound complex. A multimeric form of MukBEF would therefore allow release of one DNA segment and capture of a new segment without releasing the complex from the chromosome, a process akin to a rock climber making trial grabs to reach a hand hold, and one which could lead to ordered MukBEF movement within a chromosome, perhaps leading to DNA remodeling (fig. S1F). This is analogous to the processive "walking" of the molecular motors kinesin and dynein along microtubules (*20*). The functional advantage of dimeric SMC complex oligomerization may be exploited by other SMC complexes, irrespective of the mechanism of multimerization. Like MukBEF, bacterial SMC-ScpAB forms relatively immobile complexes that accumulate at a few chromosome positions. *Bacillus subtilis* SMC-ScpAB can form multimeric complexes in vitro, with SMC and ScpB forming homodimers and ScpA forming monomers or dimers (*15*, *21*). Eukaryote SMC complexes also share similar characteristics to MukBEF in maintaining chromosomes, accumulating at discrete chromosome loci (*22*, *23*), and turning over in seconds, as well as having the same distinctive architecture (*24*, *25*). Although they capture DNA topologically in apparent heterodimeric complexes (*26*), higher-order complexes might form and exploit the type of rock-climbing mechanism described here.

References and Notes

1. S. Gruber, *Mol. Microbiol.* **81**, 855 (2011).
2. K. Nasmyth, C. H. Haering, *Annu. Rev. Biochem.* **74**, 595 (2005).
3. A. J. Wood, A. F. Severson, B. J. Meyer, *Nat. Rev. Genet.* **11**, 391 (2010).
4. H. Niki *et al.*, *EMBO J.* **11**, 5101 (1992).
5. K. Yamanaka, T. Ogura, H. Niki, S. Hiraga, *Mol. Gen. Genet.* **250**, 241 (1996).
6. O. Danilova, R. Reyes-Lamothe, M. Pinskaya, D. Sherratt, C. Possoz, *Mol. Microbiol.* **65**, 1485 (2007).
7. S. Hiraga *et al.*, *Res. Microbiol.* **142**, 189 (1991).
8. J. S. Woo *et al.*, *Cell* **136**, 85 (2009).
9. R. Reyes-Lamothe, D. J. Sherratt, M. C. Leake, *Science* **328**, 498 (2010).
10. M. C. Leake *et al.*, *Nature* **443**, 355 (2006).
11. B. Huang, M. Bates, X. Zhuang, *Annu. Rev. Biochem.* **78**, 993 (2009).
12. Z. M. Petrushenko, C. H. Lai, V. V. Rybenkov, *J. Biol. Chem.* **281**, 34208 (2006).
13. R. Fennell-Fezzie, S. D. Gradia, D. Akey, J. M. Berger, *EMBO J.* **24**, 1921 (2005).
14. M. Gloyd, R. Ghirlando, A. Guarné, *J. Mol. Biol.* **412**, 578 (2011).
15. M. Hirano, T. Hirano, *EMBO J.* **23**, 2664 (2004).
16. B. Hu *et al.*, *Curr. Biol.* **21**, 12 (2011).
17. P. Arumugam *et al.*, *Curr. Biol.* **13**, 1941 (2003).
18. S. Weitzer, C. Lehane, F. Uhlmann, *Curr. Biol.* **13**, 1930 (2003).
19. N. Chen *et al.*, *J. Bacteriol.* **190**, 3731 (2008).
20. C. Kural *et al.*, *Science* **308**, 1469 (2005).
21. J. Mascarenhas *et al.*, *BMC Cell Biol.* **6**, 28 (2005).
22. C. D'Ambrosio, G. Kelly, K. Shirahige, F. Uhlmann, *Curr. Biol.* **18**, 1084 (2008).
23. M. T. Ocampo-Hafalla, F. Uhlmann, *J. Cell Sci.* **124**, 685 (2011).
24. D. Gerlich, T. Hirota, B. Koch, J. M. Peters, J. Ellenberg, *Curr. Biol.* **16**, 333 (2006).
25. R. A. Oliveira, S. Heidmann, C. E. Sunkel, *Chromosoma* **116**, 259 (2007).
26. C. H. Haering, A. M. Farcas, P. Arumugam, J. Metson, K. Nasmyth, *Nature* **454**, 297 (2008).

Acknowledgments: R.R.-L. held the Todd-Bird Junior Research Fellowship of New College (Oxford University). S.U. was supported by a Mathworks scholarship. M.C.L. was supported by a Royal Society University Research Fellowship. We thank R. Oliveira for assistance with FRAP experiments and A. Kapanidis for discussions and provision of the PALM equipment. The experimental work was funded by an Engineering and Physical Sciences Research Council grant to M.C.L. (EP/G061009) and by a Wellcome Trust program grant to D.J.S. (WT083469MA). All data are presented in the supplementary materials, and bacterial strains are available on request. The authors declare that they have no competing financial interests. The project was conceived by all authors, each of whom contributed to writing the manuscript. A.B., R.R.-L., and S.U. performed the experiments, M.C.L. developed the millisecond microscopy and biophysical/analytical methods, and S.U. implemented live-cell PALM. M.C.L., A.B., and S.U. did the analysis. D.J.S. and M.C.L. contributed equally.

Supplementary Materials

www.sciencemag.org/cgi/content/full/338/6106/528/DC1
Materials and Methods
Figs. S1 to S11
Tables S1 to S6
References (*27*–*46*)

9 July 2012; accepted 4 September 2012
10.1126/science.1227126